

**CALCULATION OF PERMEABILITY AND DISPERSION COEFFICIENTS IN
UNSATURATED POROUS MEDIA WITH FRACTURES - 10344**

C.K. Lee, M.Z. Htway
Handong Global University
3 Namsong-ri, Heunghae-eub, Buk-gu, Pohang, Kyungbuk, 791-708
Republic of Korea

S.P. YIM
Korea Atomic Energy Research Institute
P.O.Box 150, Yusong, Daejon, 305-600
Republic of Korea

ABSTRACT

The results of the calculation of permeability and dispersion coefficients obtained by the application of the method of homogenization for the transport of solute in an unsaturated porous medium with microscale fracture geometries are discussed. Due to sharp contrast in the viscosities of the liquid and gas phases the fluid flow takes place dominantly in the gas region. For single fracture geometries the permeability appears to be the smaller for distorted channel geometries than the straight channel geometry due to tortuosity. For multiple fractures the orientation of fractures strongly influences the permeability. The longitudinal dispersion, similar to permeability, decreases with distortion of the fracture. For multiple fracture the dispersion tensor has been calculated for two parallel straight inclined channels and various dispersion coefficients appear to be non-zero due to the fracture orientation characteristics.

INTRODUCTION

Fractures in a rock medium very often appear to be partially saturated and both the liquid(water) and gas(air) phases are present. Fluid flow in such fractures is driven by a pressure gradient over the macroscale. Since the viscosity of the air is much smaller than that of water, the air flows much more easily than the water. As a result, the solute released in a partially saturated medium will migrate dominantly with air flow.

Released solute matter experiences both molecular diffusion and hydrodynamic dispersion in the fractures of the rock medium. The non-uniform fluid velocity distribution causes enhanced spreading of solute matter by Taylor dispersion mechanism.

From the viewpoint of effective management of the underground repository located in an unsaturated rock medium it is important to evaluate the characteristics of solute transport which accompanies dispersion. In this study, the process of solute transport over the macroscale is briefly discussed in the framework of homogenization theory. Two basic assumptions are made: the heterogeneous medium structure on the microscale is periodic with periodic length l and all the variables and material properties are also periodic over the same length. The periodicity assumptions are not very restrictive because the distributions and arrangements over the periodic

length are quite arbitrary. A few boundary value problems are defined in a unit cell with side lengths equal to the period along each direction on the microscale.

The boundary value problems are solved numerically by using finite element method. The fracture domains are discretized into triangular elements. Variational principles corresponding to the microcell boundary value problems are minimized to solve for the nodal unknowns.

Several two-dimensional sample microcell geometries of fracture are chosen. For a single fracture in the unit cell a straight channel, a V-shaped channel and a S-shaped channel are chosen. For multi-fractured medium structure a unit cell with two inclined parallel straight channels inclined at 45deg from the horizontal is first considered. The parallel fractures are then connected by another straight channel. The microcell boundary value problems are then solved to determine the permeability which is required in Darcy's law and the dispersion coefficients that are required for the transport of solute matter over the macroscale.

The permeability and the dispersion coefficients are calculated for the chosen microcell geometries. For single fracture geometries the permeabilities K_{xx} (the rate of fluid movement through the medium in the x-direction due to the overall macroscale pressure gradient imposed in the x-direction) are calculated. It is smaller for V-shaped and S-shaped channel geometries due to distortion of the flow path as compared with straight channel case. For multiple channel geometries the permeability tensor has non-zero values for the off-diagonal entries K_{yx} and K_{xy} .

The dispersion coefficients D_{ij} (dispersion coefficients in i-direction due to macroscale concentration gradient in j-direction) are calculated for various fracture geometries all under the condition of macroscale pressure gradient in the x-direction. For single fractures the dispersion coefficients D_{xx} only is considered because spreading in y-direction is blocked by the rock phase allowed and the transverse dispersion becomes zero. For multiple fracture the result of dispersion coefficient calculation is shown only for two fracture medium. D_{xx} is larger than others. All of the dispersion coefficients show sharp increase with Peclet numbers larger than 30.

THE GOVERNING RELATIONS ON THE MICROSCALE

The porous medium is assumed to be composed of the matrix(Ω_m) of solid rock phase, the liquid phase(Ω_l), and the gas phase(Ω_g). It is further assumed that the liquid region exists between the rock matrix and the gas domain, and separates the two domains. Each phase is assumed to be connected throughout the porous medium. Driven by macroscopically imposed pressure gradient the fluid flow takes place dominantly in the gas region and also in the liquid region.

The basic governing equations on the microscale are summarized as follows. In Ω_f the fluid flow is governed by the conservation laws of mass and momentum and the transport of solute is governed by the mass conservation:

$$\begin{aligned} \nabla \cdot \mathbf{u} &= 0 \\ \mu \left(\frac{\partial \mathbf{u}}{\partial t} + \mathbf{u} \cdot \nabla \mathbf{u} \right) &= -\nabla p + \mu_t \nabla^2 \mathbf{u} - \mu_l g \mathbf{e}_z \\ \frac{\partial c_i}{\partial t} + \mathbf{u} \cdot \nabla c_i &= D_i \nabla^2 c_i \end{aligned}$$

where \mathbf{u} , p_l and c_l are the fluid velocity, the pressure and the solute concentration in the liquid, and ρ_l and μ_l are the density and absolute viscosity of the liquid. Also D_l is the diffusivity of the solute in the liquid.

In Ω_g ,

$$\begin{aligned} \frac{\partial \rho_g}{\partial t} + \nabla \cdot (\rho_g \mathbf{v}) &= 0 \\ \rho_g \left(\frac{\partial \mathbf{v}}{\partial t} + \mathbf{v} \cdot \nabla \mathbf{v} \right) &= -\nabla p_g + \mu_g \nabla^2 \mathbf{v} + \lambda_g \nabla(\nabla \cdot \mathbf{v}) - \rho_g g \mathbf{e}_z \\ \frac{\partial c_g}{\partial t} + \mathbf{v} \cdot \nabla c_g &= D_g \nabla^2 c_g \end{aligned}$$

in which \mathbf{v} is the fluid velocity in the gas region and other quantities with subscript symbol 'g' are defined in the same manner as in the liquid.

Although the decay effect in both phases should be accounted, it is relatively weak over the time scale of transport in the gas region and has been omitted.

On the boundary Γ between the solid and liquid, the liquid velocity vanishes and the solute flux should vanish:

$$\begin{aligned} \mathbf{u} &= 0 \\ D_l \nabla c_l \cdot \mathbf{N}^l &= 0 \end{aligned}$$

On the interface Γ_{lg} between the liquid and gas, continuity of the fluid velocity, mass flux, and Henry's law dictate that

$$\begin{aligned} \mathbf{u} &= \mathbf{v} \\ D_l \nabla c_l \cdot \mathbf{N}^l &= D_g \nabla c_g \cdot \mathbf{N}^g \\ c_g &= H c_l \end{aligned}$$

where H is Henry's law constant.

The process of deriving the macroscale governing equations is briefly summarized([1]). Two basic assumptions are introduced in the method of homogenization. First there exists a scale disparity so that there are two vastly different length scales: the microscale l and the macroscale l' . Second all the variables and material properties including the medium structure are l -periodic.

Normalization

Let l and l' be the length scales on the microscale and macroscale. They are related by

$$\frac{l}{l'} = \epsilon \ll 1$$

Also let P' and C_0 be the pressure drop over the macroscale and the reference concentration. The following normalization is introduced:

$$x = \ell x^*, t = T t^*, c_l = C_0 c_l^*, c_g = C_0 c_g^*$$

$$P_l = l^* P_l^*, P_g = l^* P_g^*, \mathbf{u} = U \mathbf{u}^* = \frac{l^* \ell^2}{\mu_l \ell^t} \mathbf{u}^*, \mathbf{v} = V \mathbf{v}^* = \frac{l^* \ell^2}{\mu_g \ell^t} \mathbf{v}^*$$

$$\frac{U}{V} = \frac{\mu_g}{\mu_l} = \delta \ll 1$$

There are several time scales: the convection time scales in the liquid and gas phases and the diffusion time scales in the liquid and gas phases which are estimated as

$$(t_v)_l = l^*/U, (t_v)_g = l^*/V, (t_d)_l = \ell^2/D_l, (t_d)_g = \ell^2/D_g$$

The diffusion time scale in the liquid is the largest one. Since the primary goal of this study is the transient process of solute transport in the gas domain, it is discarded. The order relations among other time scales are as follows:

$$(t_v)_g/(t_v)_l = \delta \ll 1, (t_v)_g/(t_d)_g = \epsilon/Pe_g = O(\epsilon), (t_v)_l/(t_d)_g = \epsilon/\alpha Pe_l = O(1)$$

The governing conditions in the dimensionless variables are omitted.

Dimensionless Parameters

The orders of magnitude of some representative dimensionless parameters are assumed as follows:

$$\text{Reynolds Number: } Re_l = \frac{U\ell}{\nu_l}, Re_g = \frac{V\ell}{\nu_g} = O(\epsilon); Re_l' = \frac{Re_l}{\epsilon}, Re_g' = \frac{Re_g}{\epsilon} = O(1)$$

$$\text{Peclet Number: } Pe_l = U\ell/D_l = O(1), Pe_g = V\ell/D_g = O(1)$$

In the above, ν_l and ν_g are the kinematic viscosities of the liquid and gas.

MULTIPLE SCALE ANALYSIS AND THE GOVERNING EQUATIONS ON THE MACROSCALE

The fast and slow coordinates are introduced for both spatial coordinates and time and the derivatives are expanded accordingly:

$$\mathbf{x}, \mathbf{x}' = \epsilon \mathbf{x} \quad ; \quad \frac{\partial}{\partial x_i} \rightarrow \frac{\partial}{\partial x_i} + \epsilon \frac{\partial}{\partial x_i'}$$

$$t_1 = t^* = l/(l_v)_g, \quad t_2 = \frac{\epsilon}{Pe_g} t_1 \quad ; \quad \frac{\partial}{\partial t} \rightarrow \frac{\partial}{\partial t_1} + \frac{\epsilon}{Pe_g} \frac{\partial}{\partial t_2}$$

The dependent variables are expanded in perturbation series:

$$f = f^{(0)} + \epsilon f^{(1)} + \epsilon^2 f^{(2)} + \dots; \quad f = \{\mathbf{v}, \mathbf{u}, p_g, p_l, c_g, c_l\}$$

At successive orders of ϵ , the following results are obtained.

(i) For fluid flow the velocity in the gas region is much larger than that in the liquid region and at leading order the gas phase behaves like an incompressible fluid:

$$p_g^{(0)} = p_g^{(0)}(\mathbf{x}^l, t_1, t_2); \nabla \cdot \mathbf{v}^{(0)} = 0$$

If the gas velocity at leading order and the first order correction of the gas pressure are expressed as

$$\begin{aligned} \mathbf{v}^{(0)} &= -\mathbf{K} \cdot (\nabla^l p_g^{(0)} + B_l c_g^{(0)} \mathbf{e}_z) \\ p_g^{(1)} &= -\mathbf{S} \cdot (\nabla^l p_g^{(0)} + B_l c_g^{(0)} \mathbf{e}_z) + p_g^{(1)} \end{aligned}$$

where the dimensionless quantity

$$B_l = \frac{C_0 g l^3}{Re_l \rho_l \nu_l^2} = O(1)$$

signifies the buoyancy effect.

The functions \mathbf{K} and \mathbf{S} must satisfy

$$\begin{aligned} \nabla^2 \mathbf{K} - \nabla \mathbf{S} + \mathbf{I} &= 0 & \text{in } \Omega_g \\ \nabla \cdot \mathbf{K} &= 0 & \text{in } \Omega_g \\ \mathbf{K} &= 0 & \text{on } \Gamma_{lg} \\ \langle \mathbf{S} \rangle &= 0 \\ \mathbf{K} \text{ and } \mathbf{S} &\text{ are } \Omega\text{- periodic.} \end{aligned}$$

where a pair of brackets is used to denote the microcell(Ω) average defined as

$$\langle f \rangle = \frac{1}{\Omega} \int_{\Omega} f d\Omega$$

It should be noted that the average is over the entire microcell, not over the gas domain only.

Darcy's law then becomes

$$\langle \mathbf{v}^{(0)} \rangle = -\langle \mathbf{K} \rangle \cdot (\nabla^l p_g^{(0)} + B_l c_g^{(0)} \mathbf{e}_z)$$

which serves as the momentum equation for the gas flow on the macroscale.

(ii) In the gas region, the solute transport is due to both convection and diffusion whereas the transport in the liquid region is due primarily to diffusion. The solute concentration in both regions are microscale independent:

$$c_g^{(0)} = c^{(0)}(\mathbf{x}^l, t_1, t_2); c_l^{(0)} = c^{(0)}(\mathbf{x}^l, t_2).$$

Over the convection time scale in the gas region,

$$\frac{\partial c_g^{(0)}}{\partial t_1} + \langle \mathbf{v}^{(0)} \rangle \cdot \nabla' c_g^{(0)} = 0$$

The first order correction of the concentration is expressed as

$$c_g^{(1)} = -\mathbf{M}^g \cdot \nabla c_g^{(0)} + \langle c_g^{(1)} \rangle$$

and the following bvp must be satisfied:

$$\begin{aligned} \epsilon' c_g (\hat{\mathbf{v}}^{(0)} - \mathbf{v}^{(0)} \cdot \nabla \mathbf{M}^g) &= \nabla'^2 \mathbf{M}^g && \text{in } \Omega_g \\ (\mathbf{I} - \nabla \mathbf{M}^g) \cdot \mathbf{N}^g &= 0 && \text{on } \Gamma_{lg} \\ \mathbf{M}^g &\text{ is } \Omega\text{-periodic.} \\ \langle \mathbf{M}^g \rangle &= 0 \end{aligned}$$

Over the diffusion time scale in the gas region,

$$\left(\frac{n_l}{H} + n_g \right) \frac{\partial c_g^{(0)}}{\partial t_2} + P \epsilon_g \frac{\alpha'}{H} \langle \mathbf{u}^{(0)} \rangle \cdot \nabla' c_g^{(0)} + P \epsilon_g (\mathbf{q} \cdot \nabla' c_g^{(0)} + \langle \mathbf{v}^{(1)} \rangle \cdot \nabla' c_g^{(0)}) = \nabla' \cdot (\mathbf{D}' \cdot \nabla' c_g^{(0)})$$

where n_l and n_g are the liquid and gas region porosity values respectively. Also

$$\alpha' = D_l / \epsilon D_g = O(1)$$

and \mathbf{q} is a convection velocity which takes a complicated form and is not given here. The dispersion tensor is given as

$$\mathbf{D}' = D_{ij} = \left\langle \frac{\partial M_i^g}{\partial x_k} \frac{\partial M_j^g}{\partial x_k} \right\rangle - \left\langle \frac{\partial M_i^g}{\partial x_j} + \frac{\partial M_j^g}{\partial x_i} \right\rangle + n_g \delta_{ij}$$

By combining the equations over the convection and diffusion time scales the macroscale transport equation becomes

$$A \frac{\partial c_g}{\partial t} + \left[\left(\frac{A}{n_g} \langle \mathbf{v}^{(0)} \rangle + \epsilon \langle \mathbf{v}^{(1)} \rangle \right) + \epsilon \frac{\delta'}{H} \langle \mathbf{u}^{(0)} \rangle + \epsilon \mathbf{q} \right] \cdot \nabla' c_g^{(0)} = \nabla' \cdot (\mathbf{D}' \cdot \nabla' c_g^{(0)})$$

The boundary-value problems summarized above must be solved to determine the permeability and dispersion coefficients for given microcell geometry.

THE MICROCELL GEOMETRIES AND NUMERICAL CALCULATION

The cell geometries used in the calculation of the permeability and the dispersion coefficients are shown in Fig. 1 and Fig. 2 together with the velocity field. The fracture domains are divided into rectangles and each rectangle is further divided into two triangular elements. Three types of single fracture geometry are chosen: a straight channel, a V-shaped channel(continuation of this is a zigzag type channel), and a sinusoidal channel. For multi-channel fracture geometry the following two types are chosen: two parallel

straight channels inclined at 45deg from the horizontal, and two parallel channels with one connecting fracture.

For selected microcell geometry the boundary-value problems can, in principle, be solved by numerical methods. Specifically finite elements have been used with quadratic basis function for the velocity and linear elements for pressure. After solving for the flow field in the fractures, the convective-diffusion problem is solved with linear basis functions. Variational principles have been derived for both the flow and convective-diffusion problems. The details are omitted here.

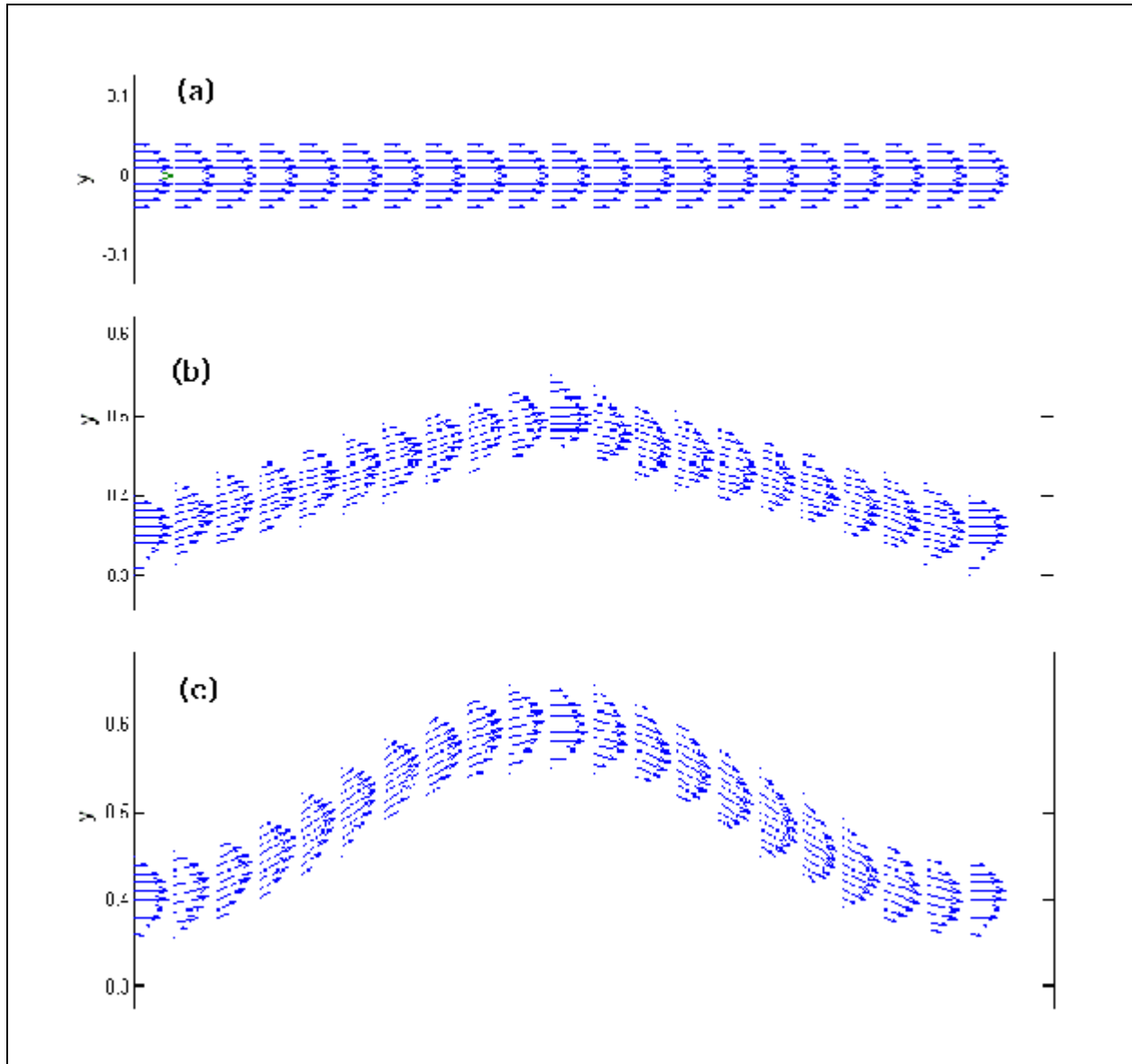


Fig. 1 The fracture geometries and the velocity fields: (a) a single straight fracture, (b) a V-shaped fracture, and (c) S-shaped fracture. The arrows show the relative magnitudes of the velocity vector.

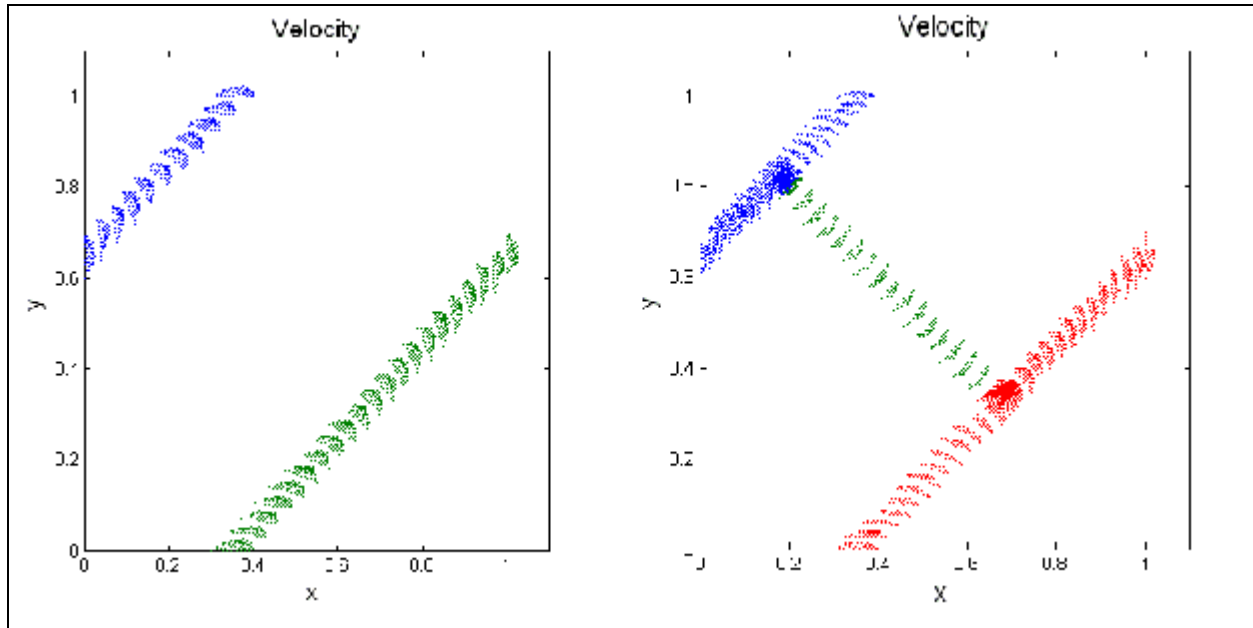


Fig. 2 The fracture geometries and the velocity fields: (a) two parallel straight fractures with an inclination from the horizontal, and (b) two parallel straight fractures with a connecting fracture. The arrows show the relative magnitudes of the velocity vector.

THE MICROCELL GEOMETRIES AND NUMERICAL CALCULATION

The cell geometries used in the calculation of the permeability and the dispersion coefficients are shown in Fig. 1. Each rectangle is further divided into two triangular elements(not shown in the figure). The cell is in square shape, i.e., if the side lengths along x- and y-directions are l_x and l_y , $l_x = l_y$.

Three types of single fracture geometry are chosen: a straight channel, a V-shaped channel(continuation of this is a zig-zag channel shape), and a S-shaped(sinusoidal) channel. For multi-channel fracture geometry the following three types are chosen: two parallel straight inclined channels, two parallel channels with one connecting fracture, and two parallel channels with two connecting fractures.

For selected microcell geometry the boundary-value problems can, in principle, be solved by numerical methods. Specifically finite elements have been used with quadratic basis function for the velocity and linear elements for pressure. After solving for the flow field in the fractures, the convective-diffusion problem is solved with linear basis functions. Variational principles have been derived for both the flow and convective-diffusion problems. The details are omitted here.

RESULTS AND DISCUSSIONS

Permeability

The sample velocity fields in the fracture are shown in Fig. 2. Because of the no-slip condition the the fracture wall, the magnitude of the velocity is zero on the wall and increases toward the central region of fracture.

Various meshes have been used to achieve convergence of the permeability. The results are summarized in Table 1 below. The symbol N_y is the number of intervals in the transverse direction across the fracture. As N_y is doubled, the permeability converges quickly. The changes from $N_y=8$ to $N_y=16$ are less than 0.1%.

For straight channel the velocity profile is parabolic across the fracture. Specifically, if the porosity of the straight channel is δ , the velocity is given as $v_x = (\delta^2/4 - y^2)/2$ from which its volume average is given as $\langle v_x \rangle = \delta^3/12$. With $\delta=0.1$ (the gas region porosity n_g is also equal to 1), it becomes $\langle v_x \rangle = 8.33330E-05$. For V-shape and S-shape channels the permeability decreases as a result of transverse distortion of the fracture as compared with the straight channel case. It is seen that the permeability is smaller for S-shape channel as the fracture is continuously distorted along the longitudinal direction.

Table 1. Permeability K_{xx} for Various Single Fractures

N_y	Straight Channel	V-shape Channel	S-shape Channel
2	8.33330 E-05	4.6027 E-05	2.5255 E-05
4	8.33330 E-05	4.6208 E-05	2.5254 E-05
8	8.33330 E-05	4.6262 E-05	2.5248 E-05
16	-	4.6291 E-05	2.5247 E-05

For multiple fracture geometries the calculated permeabilities are shown in Table 2 in which N is the number of intervals across a fracture. for two parallel fractures inclined at 45deg from the horizontal and three fracture geometry (two parallel fractures with one connecting fracture between them). Since the fractures are oriented at 45deg K_{xx} and K_{yy} values appear to be very close to each other for both cases. Also because of fracture orientations in a specific direction(non-isotropic feature) the off-diagonal entries K_{xy} and K_{yx} have non-zero values.

Table 2. Permeability for Multiple Fractures:

(a) Two Parallel Fractures

N	K_{xx}	K_{yy}	K_{xy}	K_{yx}
2	2.0985 E-05	2.0922 E-05	2.0630 E-05	2.0839 E-05
4	2.1015 E-05	2.0875 E-05	2.0609 E-05	2.0789 E-05
8	2.1020 E-05	2.0842 E-05	2.0629 E-05	2.0739 E-05

(b) Three Fractures

N	K_{xx}	K_{yy}	K_{xy}	K_{yx}
2	2.9130 E-05	2.9596 E-05	1.3820 E-05	1.3740 E-05
4	2.9192 E-05	2.9410 E-05	1.3826 E-05	1.3682 E-05
6	2.9155 E-05	2.9319 E-05	1.3522 E-05	1.3672 E-05

8	2.9111 E-05	2.9259 E-05	1.3558 E-05	1.3675 E-05
10	2.9073 E-05	2.9215 E-05	1.3500 E-05	1.1368 E-05

Dispersion Coefficients

There are two externally imposed parameters in the consideration of dispersion coefficients: one is the direction of the global pressure gradient that drives the seepage flow and the other is the direction of global concentration gradient: for the former x-direction has been chosen for convenience and the latter is specified in the second subscript in D_{ij} .

For single fracture channels, because of solute spreading in the longitudinal direction only, $D_{yx} = D_{xy} = D_{yy} = 0$. Variations of the longitudinal dispersion coefficient D_{xx} with Peclet number are shown in Fig.3(a) for the three types of channel geometries. It shows the largest for the straight channel and decreases as the geometry is changes to V-shape and then to S-shape. For the V-shape channel the dispersion in each straight segment of the fracture is similar to the straight channel case except the channel orientation, but for the S-shape channel channel orientation changes continuously all along the channel and the reduction of spreading becomes larger.

For multiple fracture geometry various dispersion coefficients are shown in Fig. 3(b) for two-channel geometry. Under the condition of macroscale pressure gradient directed into the x-axis the longitudinal dispersion coefficient D_{xx} is more than one and a half times larger than the transverse dispersion coefficient D_{yy} . It is noted that, due to the fracture orientations mainly in the direction of 45deg from the horizontal, the off-diagonal entries D_{xy} and D_{yx} are non-zero and is as large as D_{yy} . This indicates that the dispersion characteristics strongly depend on the medium structure on the microscale in terms of the fracture orientations.

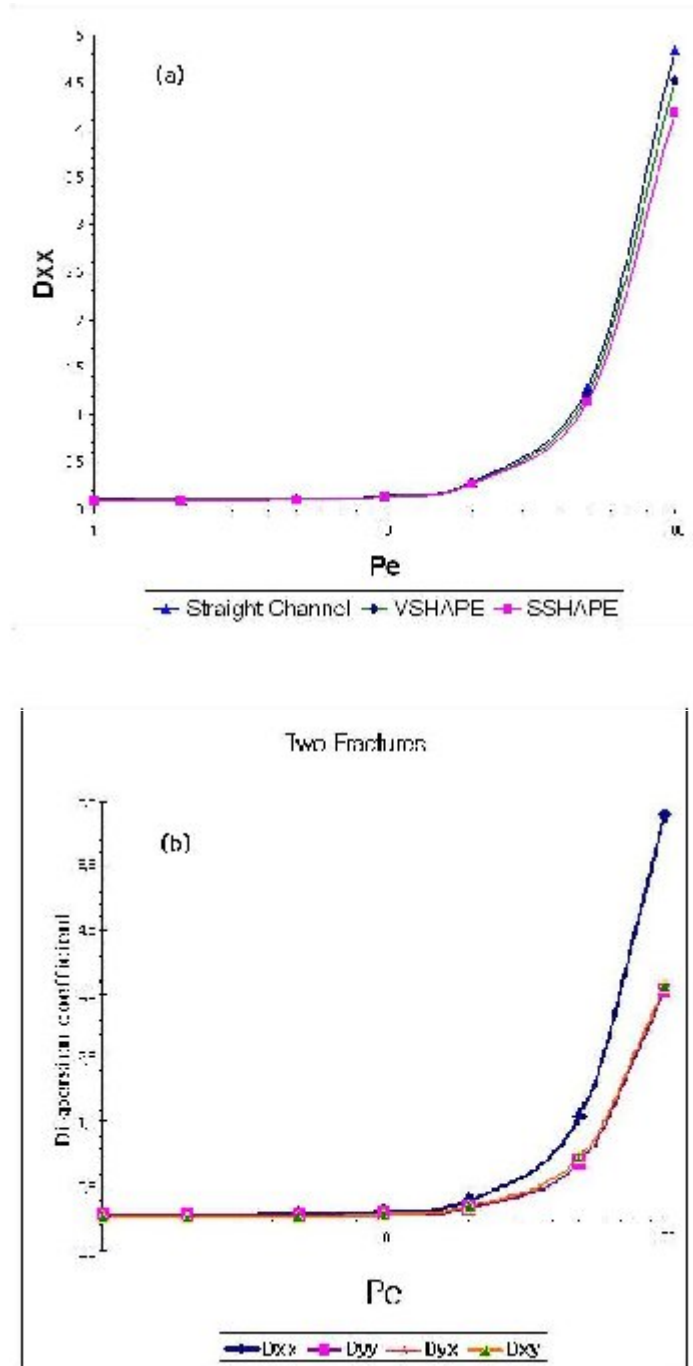


Fig. 3 The dispersion coefficients: (a) the longitudinal dispersion coefficient D_{xx} for various single fracture geometries, a straight channel, a V-shaped channel, and a S-shaped channel, (b) the dispersion coefficients D_{xx} , D_{yy} , D_{yx} , D_{xy} .

CONCLUSIONS

From the present study of calculating the permeability and dispersion coefficients for solute in an unsaturated rock medium with pores of fracture type the following conclusions are drawn.

1. The permeability for single fractures is the largest for straight channel fractures and decreases as the distortion(or tortuosity) increases..
2. The permeability for multi-fracture geometries on the microscale highly depends on the characteristics of fracture orientation. As a result seepage characteristics can hardly become isotropic and show anisotropic features to certain extent.
3. The dispersion for single fracture geometries is influenced by the flow characteristics in the fracture. As the distortion of the fracture increases, the dispersion decreases.
4. For multiple fractures the dispersion characteristics are closely related to the flow characteristics and therefore information on the fracture alignments over the microscale affect the dispersion significantly.

ACKNOWLEDGEMENT

The research reported here was supported by a grant from the Nuclear Infra Construction Program, Nuclear R&D Programs Division, Korea Science and Engineering Foundation(KOSEF). The financial support is gratefully acknowledged.

REFERENCES

1. Lee, C.K. (2008). Solute transport in an unsaturated porous medium: development of the theory by homogenization method. (in preparation).